Bioorganic & Medicinal Chemistry Letters xxx (2018) xxx–xxx

Contents lists available at ScienceDirect

Bioorganic & Medicinal Chemistry Letters

journal homepage: www.elsevier.com/locate/bmcl

Pyridazine and pyridazinone derivatives as potent and selective factor XIa inhibitors

Zilun Hu [a,*], Cailan Wang [a], Wei Han [a], Karen A. Rossi [a], Jeffrey M. Bozarth [b], Yiming Wu [b], Steven Sheriff [c], Joseph E. Myers Jr. [c], Joseph M. Luettgen [b], Dietmar A. Seiffert [c], Ruth R. Wexler [a], Mimi L. Quan [a]

[a] Bristol-Myers Squibb Company, Research and Development, 350 Carter Road, Hopewell, NJ 08540, United States
[b] Bristol-Myers Squibb Company, Research and Development, 311 Pennington-Rocky Hill Road, Pennington, NJ 08543, United States
[c] Bristol-Myers Squibb Company, Research and Development, US Rt. 206 & Province Line Road, Princeton, NJ 08540, United States

ARTICLE INFO

Article history:
Received 2 January 2018
Revised 22 February 2018
Accepted 26 February 2018
Available online xxxx

Keywords:
Factor XIa inhibitors
FXIa
Thrombosis
Pyridazine
Pyridazinone

ABSTRACT

Pyridazine and pyridazinone derivatives were designed and synthesized as coagulation factor XIa inhibitors. Potent and selective inhibitors with single digit nanomolar affinity for factor XIa were discovered. Selected inhibitors demonstrated moderate oral bioavailability.

Introduction

Evidence supports the hypothesis that factor XIa (FXIa) is a valid target for anticoagulation therapy with the promise of an increased net clinical benefit compared to currently available anticoagulants.[1–3] Preclinical, clinical,[1,3] and genetic[4] data indicates that inhibition of the intrinsic coagulation cascade FXIa is efficacious in preventing thrombosis while maintaining hemostasis. A recent clinical study showed that reducing FXI levels specifically by an antisense oligonucleotide in patients undergoing elective knee arthroplasty was an effective method for postoperative venous thromboembolism prevention and appeared to be safe with respect to the risk of bleeding.[5] Preclinical proof of concept studies demonstrated robust antithrombotic efficacy with minimal bleeding liability were reported by our group based on a series of small molecule, active site directed FXIa inhibitors.[1,6,7]

Researchers of our group have reported several series of FXIa inhibitors. The chemotypes include phenyl imidazoles,[8–10] phenyl pyridines,[11] dipeptides[12] and recently macrocycles[13] that are potent and selective FXIa inhibitors. One of the challenges with these series has been in achieving sufficient oral bioavailability. As shown in Fig. 1, the imidazole inhibitor **1** with a neutral chlorophenyltetrazole acrylamide *P*1 group had a FXIa K_i of 2.7 nM in the FXIa enzyme binding assay, and had in vitro anticoagulant activity with an $EC_{1.5x}$ of 5.3 μM in the activated partial thromboplastin time (aPTT)[8] clotting assay. However no oral bioavailability was observed for **1** in a dog pharmacokinetic study.[9] Promising oral bioavailability was observed for the phenyl pyridine and pyrimidine series by following the strategy of reducing the number of *H*-bond donors in the chemotype.[11] For example, pyridine **2** demonstrated improved bioavailability. Unfortunately these analogs were less potent than **1** in FXIa binding and aPTT clotting assays.[12] In the search for potent and orally bioavailable FXIa inhibitors, we explored and evaluated the pyridazine derived analogs (Fig. 1, A and B) based on their structural similarity to the imidazole and pyridine scaffolds, but with reduced basicity (See Fig. 2.).

The pyridazine regioisomers **3** and **4** were synthesized to compare with **2**. Table 1 shows the FXIa affinity (K_i) and in vitro anticoagulant clotting potency (aPTT $EC_{1.5x}$) for both analogs. Compounds **3** and **4** demonstrated potency comparable to the imidazole analogs[9] and better than the pyridine analog **2**[11] in the FXIa K_i and aPTT assays. The regioisomer of 4,6-disubstituted pyridazine analog (**4**, FXIa K_i = 4.1 nM) was similar in binding potency to the 3,5-disubstituted pyridazine analog (**3**, K_i = 7.0 nM), while analog **4** exhibited better aPTT potency with an aPTT $EC_{1.5x}$ of 3.5 μM than **3** (aPTT $EC_{1.5x}$ = 14 μM).

* Corresponding author.
E-mail address: zilun.hu@bms.com (Z. Hu).

https://doi.org/10.1016/j.bmcl.2018.02.049
0960-894X/

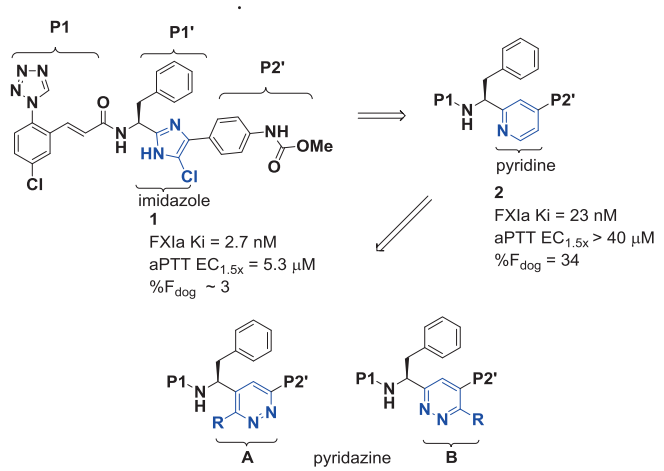

Figure 1. Pyridazine based FXIa inhibitors.

Table 1
Phenyl pyridazine FXIa inhibitors

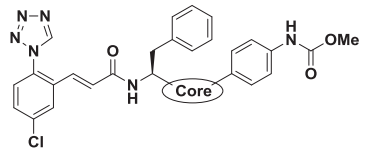

Compd	Core	FXIa K_i[a](nM)	aPTT[b]$EC_{1.5x}$(μM)
3		7.0	14
4		4.1	3.5

[a] K_i values were obtained from purified human enzyme at 25 °C and were averaged from multiple determinations ($n \geq 2$), as described in reference 8. [b]Activated partial thromboplastin time (aPTT) in vitro clotting assay was performed in human plasma as described in reference 8

A number of substituted pyridazine and pyridazinone analogs were evaluated to probe the effect on potency and metabolic stability (*infra*), and their potencies are listed in Table 2. The two pyridazinone regioisomers **5** and **6** (racemic) showed similar K_i values (10 and 22 nM) and aPTT $EC_{1.5x}$ (11 and 19 μM). Methyl substitution at the *C*3 (**7**) and *C*6 (**8**) positions also demonstrated similar potency (6.1 and 10 nM). The chlorine substitution analog at the *C*6 position (**9**) also had comparable FXIa binding (Ki = 9.6 nM) and clotting (aPTT $EC_{1.5x}$ = 9.3 μM) potencies to the *C*6 unsubstituted analog (**3**). The analog with the *C*3 chloro (**10**) was discovered to have improved potency (FXIa K_i = 1.9 nM and aPTT $EC_{1.5x}$ = 2.2 μM). Besides the methyl and chloro groups, methyl ether (**11**) and the methyl amide (**13**) analogs at the *C*6-position of the 3,5-disubstituted pyridazine were found to be less potent (FXIa K_i = 36 and 31 nM, respectively), while the carboxylic acid analog (**12**) retained FXIa potency with a K_i 11 nM.

A metabolite identification study of compounds **3** and **4** indicated that the *P*1′ phenyl group presented as a soft spot in human liver microsomes (HLM). Fluorination of the *P*1′ phenyl group provided analogs **14** and **15**, which maintained the FXIa K_i potency (Table 3). However, these modifications led to no significant improvement in HLM stability (20 and 12 min in $T_{1/2}$ for **14** and **15** versus 8.6 min for **9**). The 4-pyridine analog (**16**) demonstrated improvement in aPTT, however showed decreased HLM stability ($T_{1/2}$ 2.8 min). Selected saturated heterocyclic analogs were also evaluated. The piperidine analog **17** demonstrated weaker potency compared with **9**.

Further SAR at the *P*1′ led to the exploration of aspartic acid derivatives based on our perviously described research that the amide carbonyl made a hydrogen bond to Leu 41 of FXIa, which enhanced binding potency.[10] The introduction of aspartic amide oriented the substituent towards both the S1′ and S2 pockets, and was different from the benzyl group which projected solely into the S1′ pocket. As shown in Table 3, the hydroxypyrrolidine amide analog **18** was more potent than **17**.

Further improved FXIa binding and aPTT potencies were observed when the same *P*1′/*P*2 group was combined with the *C*3- chloropyridazine core (**19**, FXI K_i 6.6 nM and aPTT $EC_{1.5x}$

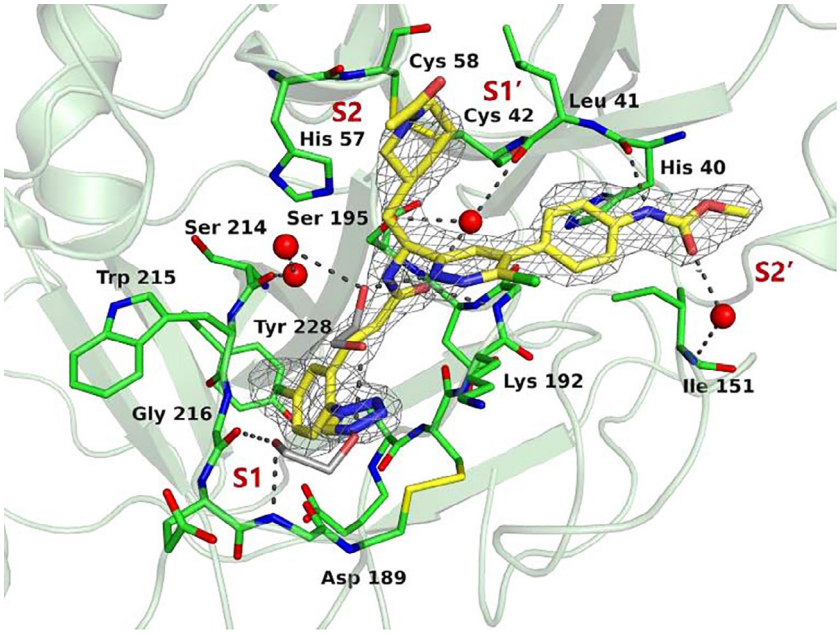

Figure 2. X-ray crystal structure of analog **17** bound to FXIa. The red spheres depict water molecules, the dotted lines depict hydrogen bonds, and ethylene diol is an artifact of the flash-cooling procedure. PDB ID: 6C0S.

Please cite this article in press as: Hu Z., et al. Bioorg. Med. Chem. Lett. (2018), https://doi.org/10.1016/j.bmcl.2018.02.049

Table 2
Substitutions on pyridazin(on)e

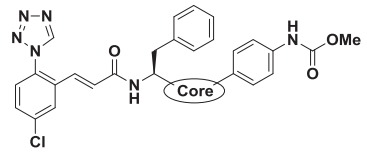

Compd	Core	FXIa Ki[a] (nM)	aPTT[b] $EC_{1.5x}$ (μM)
5		10	11
6[c]		22	19
7	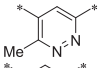	6.1	14
8	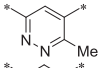	10	11
9		9.6	9.3
10	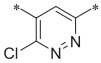	1.9	2.2
11	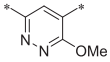	36	50
12	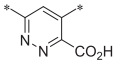	11	32
13	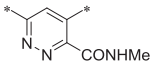	31	45

[a] K_i values were obtained from purified human enzyme at 25 °C and were averaged from multiple determinations ($n \geq 2$), as described in reference 8. [b]Activated partial thromboplastin time (aPTT) in vitro clotting assay was performed in human plasma as described in reference 8. [c]Compound **6** is racemic.

1.6 μM). The methylpiperazine amide **20** demonstrated an anticoagulant activity of aPTT $EC_{1.5x}$ 0.9 μM.

The crystal structure of compound **17** bound to the active site of FXIa was obtained at 2.35 Å resolution. This ligand shows previously observed interactions in the S1 and S2′ sites,[9–11] but also shows lipophilic interactions that lie between the S1′ and S2 pockets. The chlorophenyl tetrazole binds deep in the S1 pocket near Tyr228 and the acrylamide orients the carbonyl into the oxyanion hole formed by backbone residues Gly193, Asp194 and Ser195. One nitrogen of the chloropyridazine makes a hydrogen bond through an ethylene diol solvent molecule and a series of conserved waters to the backbone carbonyl of Ser214. As seen in preceding crystal structures of this chemotype,[9–11] the phenyl carbamate binds in the S2′ pocket, The aniline NH makes a hydrogen bond directly to the backbone of Leu41 and the carbamate carbonyl makes a hydrogen bond via a conserved water molecule to Ile151. The piperidine substituent extends towards the S1′ and S2 pocket instead of directing at the S1′ pocket that the benzyl substituents occupy. It appears the most significant interaction is van der Waals contact between the methylene of piperidine ring and residues His57, Cys58 and Cys42. Surprisingly, the carbonyl does not make any hydrogen bonds with the protein.

A representative synthesis of pyridazine *C*6-Cl and pyridazin-6-one analogs is shown in Scheme 1. The ketophosphonate (**22**) was obtained in high yield by treating dimethyl methylphosphonate with *n*-BuLi before reacting with phenylalanine derivative **21**. Condensation of **22** with ethyl 2-(4-nitrophenyl)-2-oxoacetate under basic conditions, followed by ring closing with hydrazine formed the pyridazinone **23**. The methyl carbamate was installed by nitro reduction of **23**, and then by treating the aniline **24** with methyl chloroformate to provide **25** in excellent yield. The Boc was removed from **25**, and then amide coupling with **27**[9] gave compound **5**. When intermediate **25** was treated with $POCl_3$, *C*6-chloropyridazine amine

Table 3
*P*1′ SAR of chloropyridazine

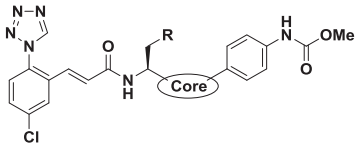

Compd	Core	R	FXIa K_i[a] (nM)	aPTT[b] $EC_{1.5x}$ (μM)
14		4-F-Ph	9.3	22
15		3-F-Ph	10	17
16		4-pyridyl	12	6.2
17			89	8.8
18			26	7.5
19	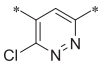		6.6	1.6
20	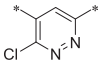	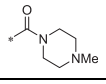	4.0	0.9

[a] K_i values were obtained from purified human enzyme at 25 °C and were averaged from multiple determinations ($n \geq 2$), as described in reference 8. [b]Activated partial thromboplastin time (aPTT) in vitro clotting assay was performed in human plasma as described in reference 8.

Please cite this article in press as: Hu Z., et al. Bioorg. Med. Chem. Lett. (2018), https://doi.org/10.1016/j.bmcl.2018.02.049

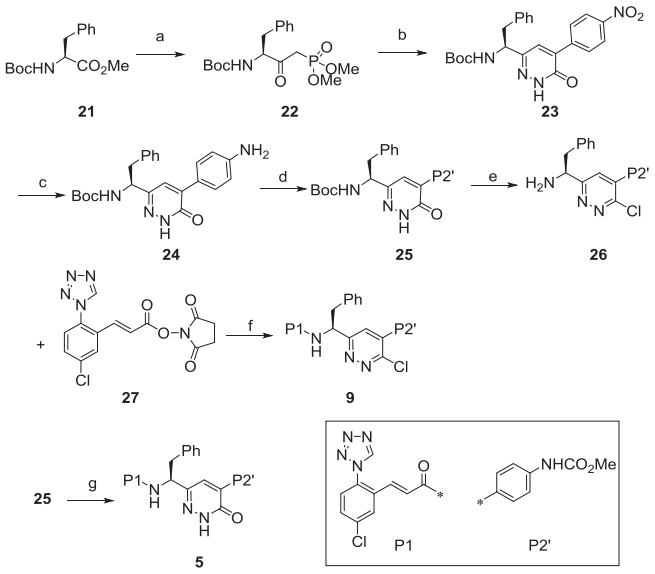

Scheme 1. Reagents and conditions: (a) dimethyl methyl phosphonate, *n*-BuLi, THF, -78 to 0 °C, 95% (b) i, ethyl 2-(4-nitrophenyl)-2-oxoacetate, K_2CO_3, EtOH, 0 °C, 30 min; ii, hydrazine, 0 °C, 20 min, 83% (c) Zn, NH_4Cl, MeOH, 100% (d) methyl chloroformate, pyridine, DCM, 0 °C, 1 h, 95% (e) $POCl_3$, acetonitrile/chloroform, 65 °C, 3 h, 78% (f) DIEA, DMF, 85% (g) i, TFA in DCM (1/1), 100%; ii, DIEA, DMF, 80%

26 was obtained, which coupled with **27** to give **9**. Other analogs with chloropyridazine core with different *P*1′ (**14**–**16**, Table 3) were prepared by following a similar procedure starting with the appropriate amino ester analogs of **21**.

Analogs of *C*6 substituted pyridazine were prepared according to Scheme 2 from intermediate **29**. Hydrogenation of **29** to remove *C*6-Cl gave *C*6-H intermediate **30**, which was converted to *C*6-H pyridazine analog **3**. The *C*6-Cl intermediate was converted to *C*6-Me via Suzuki-Miyaura cross coupling reaction, and the *C*6-Cl was also converted to C6-OMe via S_NAr reaction with NaOMe to provide **8** and **11** respectively. In addition, *C*6 carboxylation was realized through the corresponding *C*6 triflate intermediate **31** prepared from **25**, to afford ester **32**. Further functional group transformation and the installation of the *P*1 group gave compounds **12** and **13**.

The synthesis of compound **17** is outlined in Scheme 3. The protected amino ester **36** was prepared by Horner-Wittig condensation of aldehyde **33** and phosphonate **34** followed by asymmetric hydrogenation. Then by following a similar procedure as described in Scheme 1, aniline **37** was obtained, from which the *P*1 group was installed to give **38**. Methyl carbamate formation and removal of Boc provided **39**. Final acetylation and diastereomer separation by reverse phase preparative HPLC yielded **17**.

The synthesis of **18** is described in Scheme 4. By following a similar procedure as described in Scheme 1, the *tert*-butyl ester pyridazinone intermediate **41** was prepared from appropriately protected aspartic acid derivative **40**. Following steps of functional group transformations, *tert*-butyl ester **41** was converted to methyl ester **43** via acid **42**. Pyridazinone **43** was then converted to chloropyridazine followed by hydrolysis of the methyl ester to give acid **44**. Amide coupling followed by *P*1 installation provided **18**.

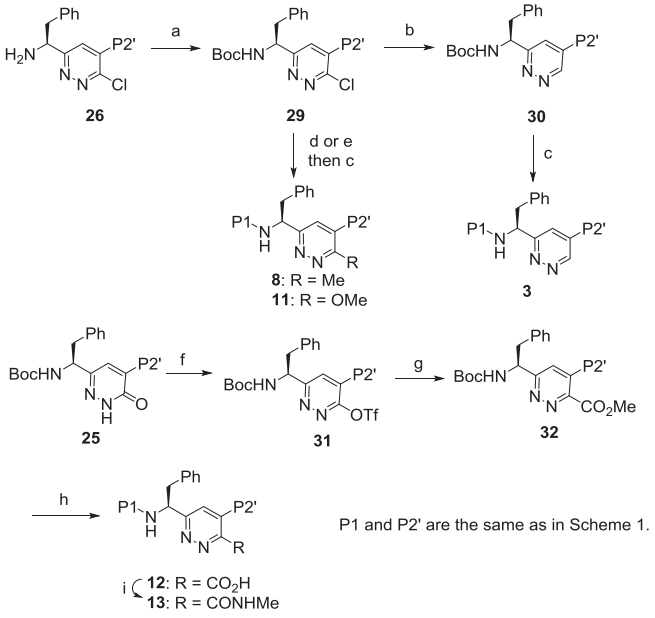

Scheme 2. Reagents and conditions: (a) Boc_2O, TEA, MeCN, 84% (b) H_2, Pd/C, MeOH, 100% (c) i, TFA, DCM; ii, **27**, DIEA, DMF, 48% for 2 steps (d) methylboronic acid, $(t\text{-}Bu_3P)_2Pd$, K_3PO_4, dioxane/H_2O, 90 °C, 54% (e) NaOMe, 91% (f) Tf_2O, pyridine, 0 °C – rt, 48% (g) CO, $Pd(OAc)_2$, DPPF, MeOH, DIEA, 55 °C, 85% (h) i, c, 85%; ii, NaOH, MeOH-H_2O, 100% (i) BOP, DIEA, DMF, 0 °C – rt, methylamine HCl salt, 95%

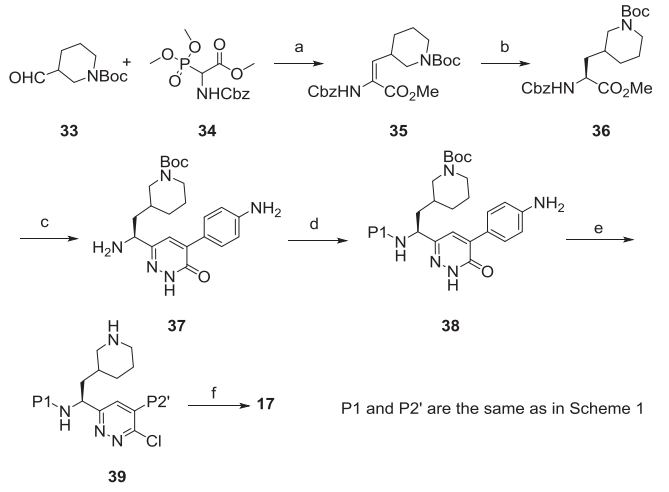

Scheme 3. (a) DBU, DCM, rt, 74% (b) (+)-1,2-bis((2*S*,5*S*)-2,5-diethyl phospholano) benzene(cyclooctadiene) rhodium (I) trifluoromethane sulfonate (1 mmol%), H_2 (50 psi), MeOH, 100% (c) Scheme 1 a–c, 25% for 3 steps (d) Scheme 1 f, 64% (e) Scheme 1d-e, 24% (f) i, AcCl, DCM/pyridine, 72%; ii, reverse HPLC separation of diastereomers.

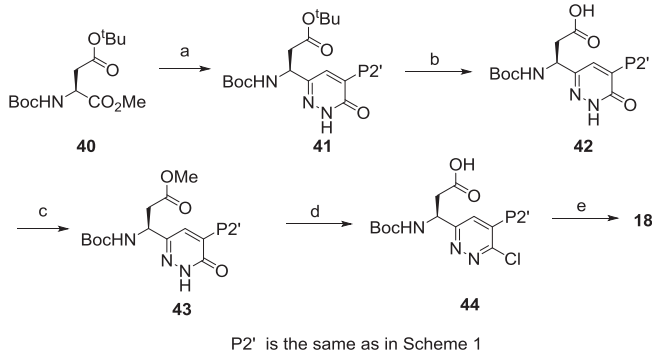

Scheme 4. Reagents and conditions: (a) Scheme 1a-d, 33% for 4 steps (b) i, TFA/DCM (1/1 v/v), rt, 1 h; ii, Boc_2O, TEA, THF/H_2O, 97% for two steps (c) $TMSCH_2N_2$, DCM, MeOH, 100% (d) i, $POCl_3$, $CHCl_3$; ii, Boc_2O, TEA/DCM; iii, LiOH, THF/H_2O, 55% for three steps (e) i, (*R*)-pyrrolidin-3-ol HCl salt, PyBOP, DIEA, DMF, 88%; ii, TFA/DCM, rt; iii, **28**, DIEA, DMF, rt, 80%

The analogs with *C*3-Cl and other substitutions were prepared according to Scheme 5. By utilizing a modified Minisci procedure,[14] alkylation of 3,6-dichloropyridazine with either Cbz or phthalimide (Phth) protected amino acids afforded 4-substituted-3,6-dichloropyridazine **45**–**47**. While preparing **47**, the hydrolyzed product **48** was obtained as well in low yield. Suzuki coupling to introduce 4-methyl carbamoylphenyl *P*2′ group gave intermediates **49**–**51**. The protecting groups were removed to afford amines **52** and **53**. The racemic amines **52** and **53** were resolved by chiral SFC chromatography, and the enantiomerically pure amines were coupled with **27** to afford **10** and **54**. By following a similar procedure, **48** was converted to *C*3-pyridazinone analog **6**. From **54**, the *P*1′ amide analogs (**19**–**20**) were obtained by following a similar synthesis as described in Scheme 1. Intermediate **51** was converted to product **4** and **7** as described in the Scheme 5.

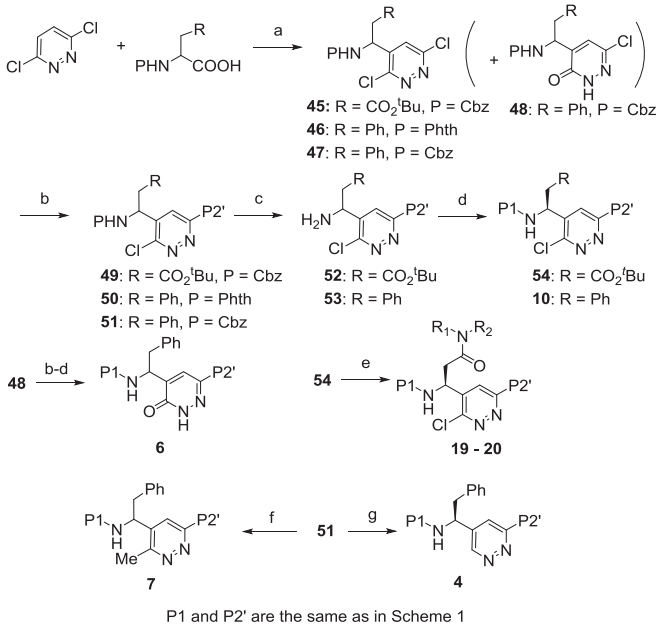

Scheme 5. Reagents and conditions: (a) $(NH_4)_2S_2O_8$, $AgNO_3$, TFA, H_2O, 75 °C, 13% (**45**); 23% (**46**); 18% (**47**) and 5% (**48**) (b) (4-((methoxycarbonyl) amino)phenyl) boronic acid, $Pd_2(dba)_3$, *t*-Bu_3P, Cs_2CO_3, dioxane, 90 °C, 31% (**49**); 41% (**50**); 45% (**51**) (c) H_2, Pd/C, MeOH, 84% for **49** and 90% for **51**; or hydrazine, EtOH, 73% for **50** (d) i, Chiralcel OD, eluted with 80% EtOH-MeOH (1:1) - 20% heptane ii, **27**, DIEA, DMF, rt, 16 h, for **54**, 68%; for **10**, 70% (e) i, TFA, DCM, 100%; ii, isobutylchloroformate, DIEA, DMF, amine, 0 °C – rt, 95% (f) i, methylboronic acid, $(t\text{-}Bu_3P)_2Pd$, K_3PO_4, dioxane, 90 °C, 55% ii, c and d-ii (g) i, H_2, MeOH, 100% ii, d, 80%

The selectivity profiles of representative pyridazine FXIa inhibitors are listed in Table 5. These compounds are highly selective against a panel of relevant serine proteases. Compounds **3**, **9** and **10** demonstrated some weak activity against FXa and/or plasma kallikrein

In summary, derivatives of pyridazine and pyridazinone were identified as potent and selective FXIa inhibitors. Among these FXIa inhibitors, *C*3-(un)substituted derivatives were more potent than

Pharmacokinetic profiles of selected compounds were evaluated in dogs using cassette dosing, and the results are listed in Table 4.

The more potent *C*3-(un)substituted pyridazine regioisomers with phenyl and amide *P*1′ groups (**4**, **10** and **19**) demonstrated moderate clearance and volume of distribution. No oral bioavailability was observed even though improved HLM stability were observed for **10** and **19**. The *C*6-(un)substituted pyridazine derivatives (**3**, **8**, **9** and **14**), demonstrated moderate oral exposure with bioavailability ranging from 12 to 18%. Low clearance, low to moderate volume of distribution and slightly longer half-lives were observed. Even though permeability (Caco-2 or PAMPA, data not shown) of these compounds was not affirmative to draw a conclusion due to poor solubility for some of them, the intramolecular *H*-bonding of the *N3*-nitrogen with the amide NH of *P*1 linker could enhance permeability, and therefore improve oral bioavailability.

Table 4
PK profiles of selected compounds[a]

Compd	Cl (mL/min/kg)	Vdss (L/kg)	$t_{1/2}$ (h)	F (%)	HLM $T^b_{1/2}$ (min)
4	18.2	1.4	1.1	<3	9.6
10	15.5	2.1	1.8	<3	31
19	24.7	1.2	0.9	<3	36
3	8.9	1.3	1.8	18	9.1
8	9.2	1.2	2.0	14	5.1
9	6.3	2.3	7.1	16	8.6
14	5.1	1.5	6.7	12	20

[a] Compounds were dosed at 0.2–0.5 mg/kg po, and 0.2–0.4 mg/kg iv dosing in a cassette format; dosing vehicles: 10% DMAC - 10% EtOH -10% PG -70% water for iv, and 10% EtOH - 70% PEG400 - 20% TPGS for po. [b]Human liver microsome half-life (HLM $T_{1/2}$) of compounds were determined by following the method described in Ref. 15

Table 5
Human Serine Protease Selectivity Profile for **3**, **8**, **9** and **10.**

Human Enzyme Ki (nM)[a]	**3**	**8**	**9**	**10**
Factor XIa	7.0	10	9.6	1.9
Factor VIIa	>13300	>13300	>13300	3280
Factor IXa	NT[b]	39,300	>73700	22,000
Factor Xa	840	>3000	200	1940
Thrombin	>13300	>13300	>13300	10,600
Trypsin	>6220	>6220	>6220	3730
Plasma Kallikrein	268	1370	>6000	192
Activated Protein C	68,000	>64400	>64400	16,300
Plasmin	38,100	>53400	76,600	4490
TPA	>14700	>14700	10,100	994
Urokinase	>29730	>29730	>29730	13,330
Chymotrypsin	11,900	>27200	>27200	29,600

[a] All Ki values in nM were obtained using human purified enzymes. [b]Not tested

*C*6-(un)substituted isomers. The *C*6-(un)substituted pyridazine derivatives demonstrated moderate oral bioavailability in pharmacokinetic studies in dogs.

Acknowledgments

The authors would like to thank Dr. James R. Corte and Dr. William R. Ewing for helpful discussions and review of the manuscript.

A. Supplementary data

Supplementary data associated with this article can be found, in the online version, at https://doi.org/10.1016/j.bmcl.2018.02.049.

References

1. (a) Pinto DJP, Orwat MJ, Smith II LM, et al. *J Med Chem*. 2017. https://doi.org/10.1021/acs.jmedchem.7b01171;
(b) Bane CE, Gailani D. *Drug Discovery Today*. 2014;19:1454–1458.
2. Schumacher WA, Luettgen JM, Quan ML, Seiffert DA. *Arterioscler Thromb Vasc Biol*. 2010;30:388.
3. (a) Yamashita A, Nishihira K, Kitazawa T, et al. *J Thromb Haemost*. 2006;4:1496–1501;
(b) Tucker EI, Marzec UM, White TC, et al. *Blood*. 2009;113:936–944;
(c) Gruber A, Hanson SR. *Blood*. 2003;102:953–955;
(d) Crosby JR, Marzec U, Revenko AS, et al. *Arterioscler Thromb Vasc Biol*. 2013;33:1670–1678;
(e) Zhang H, Lowenberg EC, Crosby JR, et al. *Blood*. 2010;116:4684–4692.
4. (a) Salomon O, Steinberg DM, Koren-Morag N, Tanne D, Seligsohn U. *Blood*. 2008;111:4113–4117;
(b) Salomon O, Steinberg DM, Dardik R, et al. *J Thromb Haemost*. 2003;1:658–661;
(c) Salomon O, Steinberg DM, Zucker M, Varon D, Zivelin A, Seligsohn U. *Thromb Haemost*. 2011;105:269–273;
(d) Doggen CJM, Rosendaal FR, Meijers JCM. *Blood*. 2006;108:4045–4051;
(e) Meijers JCM, Tekelenburg WLH, Bouma BN, Bertina RM, Rosendaal FR. *N Eng J Med*. 2000;342:696–701.
5. Buller HR, Bethune C, Bhanot S, et al. *N Engl J Med*. 2015;372:232–240.
6. Quan ML, Wong PC, Wang C, et al. *Med Chem*. 2014;57(3):955–969. (b) Wong PC, Quan ML, Watson CA, et al. *Thromb Thrombolysis*. 2015;40(4):416–423.
7. Wong PC, Quan ML, Watson CA, et al. *Thromb Thrombolysis*. 2015;40:416–423.
8. EC1.5x is defined as the plasma concentration of FXIa inhibitor required to increase aPTT to 1.5-times baseline. See: Hangeland JJ, Friends TJ, Rossi KA, et al. *J Med Chem*. 2014;57:9915–9932.
9. Pinto DJP, Smallheer JM, Corte JR, et al. *Bioorg Med Chem Lett*. 2015;25:1635–1642.
10. Hu Z, Wong PC, Gilligan PJ, et al. *ACS Med Chem Lett*. 2015;6:590.
11. (a) Corte JR, Fang T, Hangeland JJ, et al. *Bioorg Med Chem Lett*. 2015;25:925–930;
(b) Corte JR, Fang T, Pinto DJP, et al. *Bioorg Med Chem*. 2016;24:2257–2272.
12. Smith II LM, Orwat MJ, Corte JR, et al. *Bioorg Med Chem Lett*. 2016;26:472–478.
13. (a) Corte JR, Yang W, Fang T, et al. *Bioorg Med Chem Lett*. 2017;27:3833–3839;
(b) Wang C, Corte JR, Rossi KA, et al. *Bioorg Med Chem Lett*. 2017;27:4056–4060.
14. Cowden CJ. *Org Lett*. 2003;5:4494–4499.
15. McNaney CA, Dexler DM, Hnatyshyn SY, et al. *Assay Drug Dev Technol*. 2008;6:121–129.